

Low-Cost Coir Fiber Composite with Integrated Strength and Toughness

Fengyun Guo,[†] Nü Wang,^{*,†} Qunfeng Cheng,[†] Lanlan Hou,[†] Jingchong Liu,[†] Yanlei Yu,[‡] and Yong Zhao^{*,†}

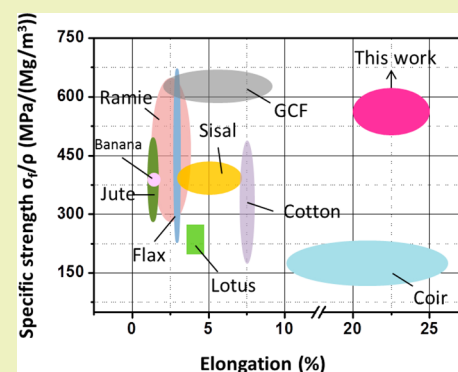
[†]Key Laboratory of Bioinspired Smart Interfacial Science and Technology of Ministry of Education, Beijing Key Laboratory of Bioinspired Energy Materials and Devices, School of Chemistry and Environment, Beihang University, Beijing 100191, China

[‡]Department of Materials Science and State Key Laboratory of Molecular Engineering of Polymers, Fudan University, 220 Handan Road, Shanghai 200433, China

S Supporting Information

ABSTRACT: With the growing environmental problems and depletion of petroleum resources, there is an urgent demand for the biorenewable, sustainable, and environmentally friendly composite materials. Here, we report a green coir fiber composite with specific mechanical properties superior to that of other reported natural fiber/polymer composites. After treatment, both strength and toughness of the composite fiber were substantially improved (91.13% and 175.7% higher than that of untreated counterpart), where exposed cellulose nanofibrils and stacking layer formed by NaOH infusion and the hydroxyl-containing hydrophilic poly(vinyl alcohol) coating play a crucial role in physicochemical interaction and thereby mechanical enhancement. By observing the process of the micro/nanostructure evolution, the strengthened mechanism from nanoscale to macroscale was demonstrated. We believe that this strategy could open new insights into the design of strong and sustainable composite fiber for further practical applications, such as textile, home furnishings, and industrial products.

KEYWORDS: Green composite fibers, Mechanical properties, Multiscale hierarchical structure, Synergetic enhancement, Cellulose nanofibrils



INTRODUCTION

With the development of the petrochemical industry, synthetic plastics are playing an increasingly important part in a diverse range of applications in modern society. Numerous non-degradable synthetic materials have been developed and utilized in the past decades, which accompany a serious depletion of resources and deterioration of the environment. At the same time, many renewable biomass wastes were often discarded without effective utilization, which results in huge resource waste as well as water eutrophication. Due to the ever-increasing environmental awareness, the past few years have witnessed a substantial shift in the development of green composites using common materials as an alternative to conventional nondegradable plastics derived from petroleum resources.¹ Besides human-engineered biodegradable polymers such as poly(lactic acid) or polyurethane,² environmentally friendly and sustainable green composites derived from natural materials have also received increasing attention,³ such as cucumber vine,⁴ lotus fiber,⁵ feather,⁶ cotton,⁷ towel gourd tendrils,⁸ hemp,⁹ winter melon,¹⁰ bamboo,¹¹ and spider silk and silkworm cocoons,¹² which mainly involve the study of structure, mechanical properties, and various applications.¹³ Since the mechanical property is a fundamental prerequisite for

practical applications, numerous studies have been carried out to study their improvement using various methods including twist,⁵ post-treatment, and integral extrusion and drawing process.¹⁴ However, the practical application of these materials is hindered by various conceivable shortcoming, as they are usually fragile, inaccessible, complicated in terms of the method, or size-inappropriate.

As an alternative to prepare green composites, coir fibers, growing mainly in tropical regions, born with the ability to withstand the harsh typhoon environment while remaining intact and seldom breaking, offer a path toward solving the challenge of designing materials that are both strong and tough.¹⁵ In particular, coir fibers, often discarded or unemployed in our life,¹⁶ have great advantages compared with the materials mentioned above especially for the preparation of strong green composites as they are low-cost, lightweight, sustainable, and easy-to-get, and have available applicable dimensions and outstanding mechanical properties.¹⁷ Thus, many foresighted attempts have been taken to fabricate

Received: April 21, 2016

Revised: August 16, 2016

Published: August 18, 2016

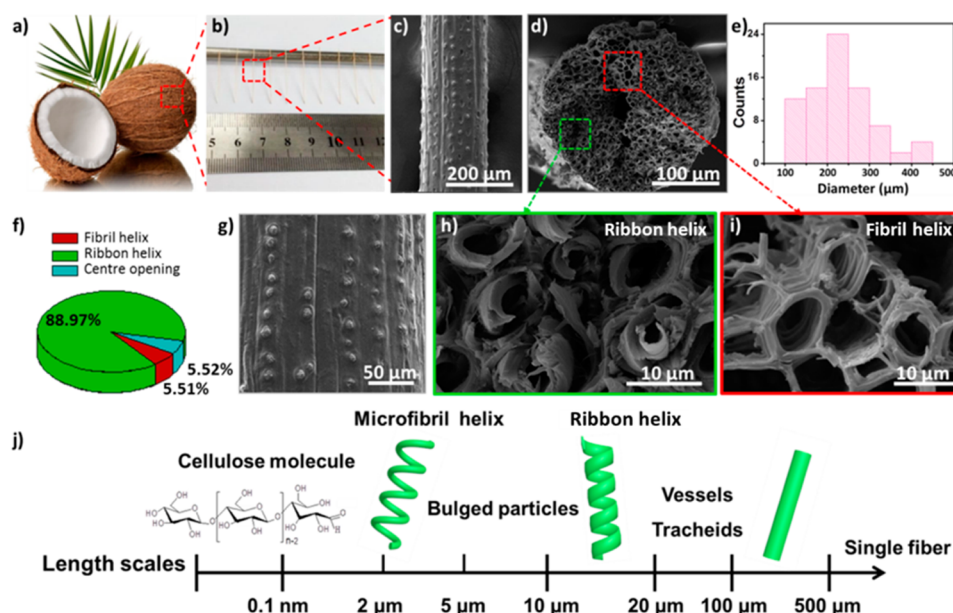


Figure 1. Multiscale hierarchically structures of natural coir fiber. (a) Natural coconut. (b) Coir fibers collected from coconut shell. (c, d) Close view and cross section of a single fiber. (e) The diameter distribution of the coir fibers with a range 120–440 μm , and the average diameter is 210 μm . (f) Relative area ratios of fibril helix, ribbon helix, and center opening. (g) SEM image of magnified surface appearance. (h) Spiral structure assembled by coiled ribbon helix. (i) Honeycomb structure assembled by coiled fibril helix. (j) Length scales of multiscale hierarchical microstructure in a single coir fiber.

materials using coir fibers as reinforcement, such as coir/PP,¹⁸ coir/PBS,¹⁹ and coir/polyester.²⁰ In these works, researchers mainly focused on improving the strength of the bulk composite resins by directly mixing coir fibers into resins. The target materials mostly involved in fiber reinforced resin with various fiber embedded in the polymer by means of a physical hot-pressing method. Nevertheless, the mechanical performance of such coir composites is still not satisfactory. Therefore, understanding how the composition and structure affect the mechanical properties was primarily significant and important especially for the single green fiber consisting of natural fiber and polymer, but rarely reported. Also, the basic mechanism of interaction between natural fibers and polymers remained unverified and elusive. Herein, we fabricated a green coir fiber composite with integrated strength and toughness by a very simple, low-cost, alkali, and poly(vinyl alcohol) treatment. The perfect construction and chemical interaction between substrate and additive result in 91.13% and 175.7% improvement on strength and toughness, which are higher than those of other reported natural fiber/polymer composites.^{2,5} Our methodology opens a new way to engineer a cost-effective green composite and thereby extend the range of applications.

EXPERIMENTAL SECTION

Materials. PVA (powder, $(\text{C}_2\text{H}_3\text{OH})_n$, $M_w = 89\,000$ – $98\,000$, 99+ % hydrolyzed) was purchased from Aldrich and used as received. NaOH and ethanol were of analytical reagent grade and purchased from Beijing Chemical Works. The coir fiber was collected from coconut shell grown from Hainan, China. The diameters of single coir fiber distribute in a range 120–440 μm , and the average diameter is 210 μm .

Preparation of Composite Fiber. The pure coir fibers were first soaked in NaOH solution (20 mL) with concentration of 1, 5, and 10 wt % for 17 h at room temperature. Afterward, the NaOH infused coir fibers were dried in air for 1 h and then washed with distilled water and ethanol to remove residual ions. The NaOH treated coir fibers were then immersed in a bath containing PVA with desired concentration

(5 wt %) for 2 h to enable the interaction between PVA and coir fiber. Upon completion of PVA coating and infusion, the composite fibers were put in the oven at 40 $^{\circ}\text{C}$ for 10 min and then air-dried. The as-prepared single green composite fibers were cut into short fibers for a subsequent experiment. The sketch of fabrication process for coir composite fiber is displayed in Figure 2a.

Characterization. Scanning electron microscopy images were taken by the Quanta 250 FEG. In order to ensure the accuracy, Quanta 250 FEG and Digital Caliper (0–150 mm) were used to measure the diameter of the fiber. IR spectra were collected using a Nicolet-iN10MX spectrometer in the FTIR mode. Tensile mechanical properties were evaluated at room temperature (25 $^{\circ}\text{C}$) using a Shimadzu AGS-X Tester with a 100 N force cell at a loading rate of 1 mm/min. The samples were cut with the length of 15 mm. A gauge length of 5 mm was used. We selected 20 fibers for testing. The average values were obtained by measuring at least five typical samples. Also, the results of stress–strain curves, strength, modulus, and elongation were calculated from load–displacement curves.

RESULTS AND DISCUSSION

The coir composite fiber with excellent mechanical property was fabricated by a NaOH treatment and poly(vinyl alcohol) (PVA) infusion method. In order to obtain a composite fiber with desirable properties, a deeper understanding of the multilevel microstructure of natural coir fiber is needed and primarily important. Therefore, we first examine the configuration and structure at multiple length scales, from the molecular to the macroscopic. Figure 1a,b are coir fibers collected from a coconut shell. Figure 1c shows scanning electron microscope (SEM) images of single fiber. The corresponding cross section of a single fiber was shown in Figure 1d. The circular and elliptical pores are orderly arranged around a center opening. The diameter of coir fibers distribute at a range 120–440 μm , and the average diameter is about 210 μm (Figure 1e). Figure 1g shows magnified SEM images of surface morphology. Typical multiscale hierarchical structure of coir fiber at the cross section are shown in Figure 1h,i. Figure

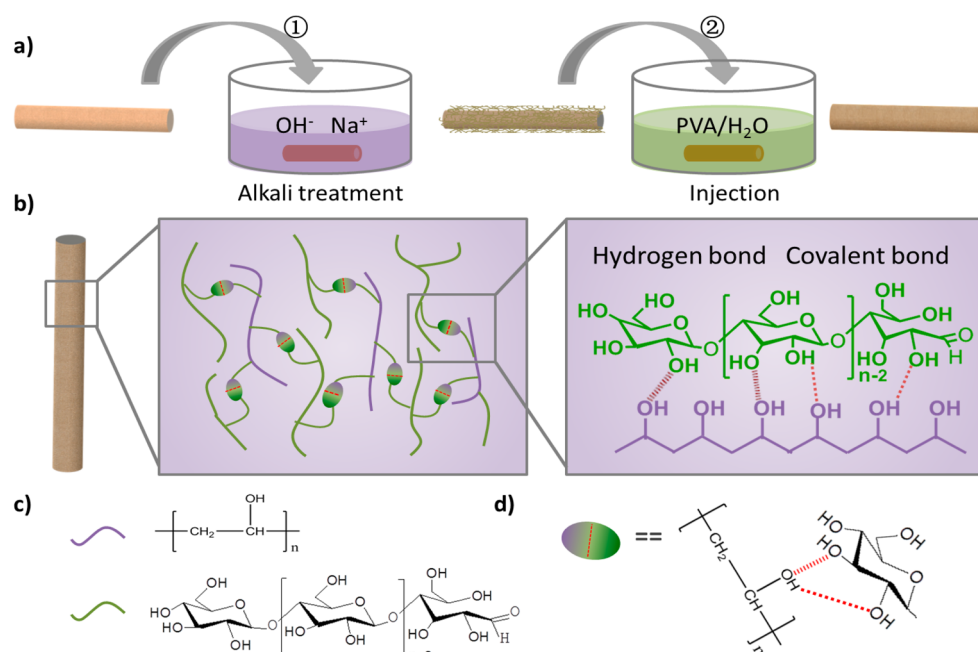


Figure 2. Illustrations of the preparation process and chemical modification mechanism for the composite coir fiber. (a) First, the coir fiber is immersed in NaOH/H₂O solution. Then, alkali treated fiber is washed by purified water and ethyl alcohol followed by injection with PVA/H₂O solution. After air-drying, the PVA-coated green composite fibers were obtained. (b–d) Proposed structural model and interaction between substrate and additive.

1g reveals significantly parallel groove and globular particles coating the pits on the cell walls that are embedded in the fiber surface. With a close-up view, the spiral ribbon configuration (Figure 1h) and coiled microfibril structure (Figure 1i) are obvious, which are orderly assembled in the form of vessels and tracheids with the shape of a helix. The relative area ratio of the fibril helix and ribbon helix were calculated and determined to be 5.51% and 88.97%, and the remaining 5.52% is the center opening (Figure 1f). Figure 1j shows length scales of microstructure in a single coir fiber. Generally, there exist at least five kinds of microstructures inside the fiber, namely, cellulose molecules (nanometer), spring-like microfibrils (about 2 μ m), bulged particles (about 8 μ m), helix ribbon (about 13 μ m), and cylindrical tracheid (about 60 μ m). At the nanoscale, the helix ribbon and microfibrils helix, two typical structures in the fiber, are mainly made up of cellulose molecules. Then, the helices aligned side by side, assembling into vessels and tracheids. Finally, these vessels and tracheids further assemble into a macroscopic coir fiber. In brief, the coir fiber has a typical multiscale hierarchical structure from the nanoscale to the macroscopic scale. This perfect self-assembled configuration endowed by nature provides thoughts for subsequent material design and provides a guarantee for performance improvement.

As a part of reinforcement in the composite, the mechanical properties of single coir fibers play a crucial role in improving integrated performance. Therefore, how to maximize and optimize mechanical strength of a single fiber is particularly important. Previous reports have suggested that alkali treatment is a relatively effective method for improving mechanical properties of fiber reinforced bulk materials.^{21,22} In this work, we demonstrated that alkali combined with hydroxyl-containing PVA could further significantly strengthen the performance of a single fiber. Figure 2 shows the preparation process and chemical modification mechanism of green coir composite fibers. The coir fibers were first immersed in NaOH aqueous

solution with different concentrations. After being washed by purified water and ethyl alcohol, alkali treated fibers were immersed into PVA aqueous solution (Figure 2a). After drying, coir composite fibers were obtained. Figure 2b–d shows the proposed chemical modification enhancement mechanism. Alkali plays three roles in this treatment, that are cleaning fiber surface, promoting mechanical interlocking between cellulose fibril through hydrogen bonding, and improving hydrophilicity of the fiber. The treated coir fibers form a compatible interface and thereby facilitate chemical interaction between fiber and PVA through good interfacial adhesion, covalent bonds, and hydrogen bonds (SEM image in Figure S1 denoted by red box and IR spectrum in Figure S2 denoted by rectangle shading). In this simple treatment process, only a small amount of low concentration NaOH and biodegradable PVA are used; it is, therefore, a very low-cost process, and the as-obtained coir composite fibers are green materials.

Figure 3 summarized the mechanical properties of as-prepared green coir composite single fibers in different conditions. Figure 3a shows representative stress–strain curves of untreated coir fiber, NaOH treated coir fiber, and PVA/NaOH treated coir fiber. The concentration was optimized (1% NaOH and 5% PVA) and selected on the basis of Figure S3, in which the tensile strength of the fiber at first increased and then decreased as the concentration of NaOH increased. The addition of NaOH changes the morphology of fiber and the arrangement of units in the cellulose macromolecule. The maximum strength is obtained at a concentration of 1%. From the stress–strain curve (Figure 3a), we can see that the coir composite fiber showed linear elasticity with a steep slope at low strains before the turning point, a plastic region with a gradual stress increase in response to a large deformation, and a breaking point at the largest strain (Figure 3a). The tensile strength, toughness, and modulus of the untreated coir fiber were 332.41 ± 36.22 MPa, 30.15 ± 9.17 MJ m^{−3}, and $6.36 \pm$

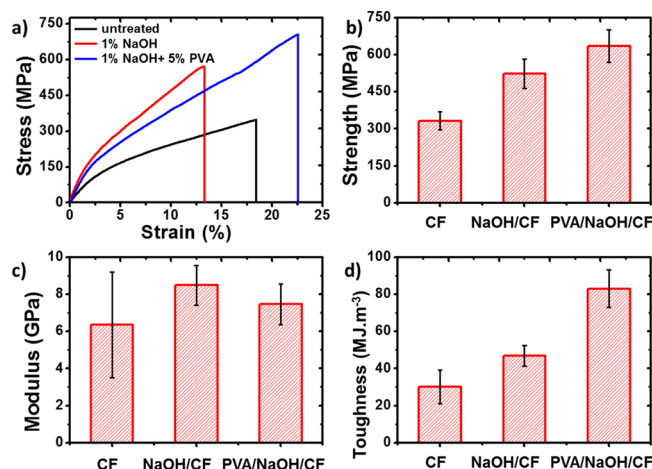


Figure 3. Mechanical properties of as-prepared coir composite fibers in different conditions. (a) Representative stress–strain curves of untreated coir fiber, NaOH treated coir fiber, and PVA/NaOH treated coir fiber. (b–d) The strength, modulus, and toughness calculated from part a. The results reveal that, upon treatment with NaOH (1 wt %) and PVA (5 wt %), the tensile strength, toughness, and modulus of fiber were significantly increased up to 635.36 ± 66.60 MPa, 83.14 ± 10.02 MJ m⁻³, and 7.46 ± 1.10 MPa (increased by 91.13% and 175.7% in strength and toughness compared with untreated coir fiber).

2.85 MPa, respectively, which are within a similar order of magnitude as compared to previously reported values.² However, after NaOH treatment, the tensile strength, toughness, and modulus had changed to 523.12 ± 59.20 MPa, 46.90 ± 5.60 MJ m⁻³, and 8.50 ± 1.07 MPa, which is 57.37% and 33.65% larger than those of a pure coir fiber in terms of strength and modulus. However, it is noticed that the tensile strain decrease. In a combination with NaOH (1 wt %) and PVA (5 wt %), with PVA mass content of 6.8% (w/w), the tensile strength, toughness, and modulus were significantly increased up to 635.36 ± 66.60 MPa, 83.14 ± 10.02 MJ m⁻³, and 7.46 ± 1.10 MPa (increased by 91.13% and 175.7% in strength and toughness compared with the untreated coir fiber), as shown in Figure 3b–d. That means that a coir/PVA composite fiber with strong integrated strength and toughness was obtained. Mechanical properties of fiber and composite in table format are shown in Table 1.

Table 1. Mechanical Properties of Fiber and Composite

specimen	strength (MPa)	toughness (MJ m ⁻³)	modulus (MPa)
coir fiber (CF)	332.41 ± 36.22	30.15 ± 9.17	6.36 ± 2.85
NaOH/CF	523.12 ± 59.20	46.90 ± 5.60	8.50 ± 1.07
PVA/NaOH/CF	635.36 ± 66.60	83.14 ± 10.02	7.46 ± 1.10

In order to understand and illuminate the mechanical enhancement mechanism, we characterized the morphology of fibers after NaOH and PVA treatment (Figure 4). Figure 4a–d shows fibers' surface morphology with alkali concentrations of 1, 5, and 10 wt %, respectively. With the concentration increasing, the microscopic surface topography varies (Figure S4); the colors of the fiber change into dark yellow and finally to brown because of the light reflection and transmission channel formed after liquid immersion. The reason is that the liquid absorption along with Na⁺ and OH⁻ is increased with gradually enhanced roughness and porosity due

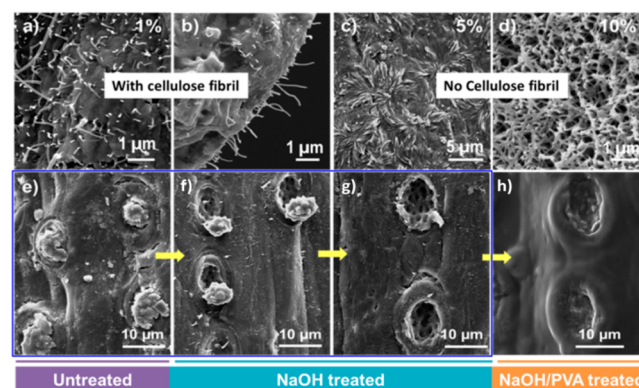


Figure 4. Morphology of coir fiber after alkali and PVA treatment. SEM images of exposed cellulose nanofibrils [1 wt % NaOH, (a) surface and (b) cross section], (c) flower clusters (5 wt % NaOH), and (d) porous fibrous network (10 wt % NaOH). (e–g) The process of globular particle removal after NaOH treatment and (h) final PVA coating. With alkali treatment, globular particles covered on fiber surface are removed and elliptical pits are exposed, leading to increased surface roughness. Thus, PVA solution could infuse and permeate through the uncovered pits, making an improved interface effect.

to the microstructure change from cellulose nanofibrils to flower clusters and finally to a porous fibrous network. With the concentration ever-increasing, the fiber is eroded, thereby leading to a darker color. When the concentrations of NaOH were 1 wt %, cellulose nanofibrils were exposed in the surface (Figure 4a) and corresponding cross section (Figure 4b). If the concentration of NaOH was increased to 5 wt %, flower clusters formed (Figure 4c). The structure further changed to a porous fibrous network structure if the NaOH was increased to 10 wt % (Figure 4d). Among this, what should be noted especially is the exposed cellulose nanofibril structure obtained through 1 wt % alkali treatment, as it is responsible for subsequent interfacial interaction and mechanical enhancement through chemical cross-linking with PVA. Figure 4e–g shows the process for globular particles that are removed after NaOH treatment, and the final PVA coating (Figure 4h). After alkali treatment, globular particles covered on fiber surface are removed gradually, and elliptical pits are exposed, leading to increased surface roughness. Then, the PVA solution could infuse and permeate through the uncovered pits, forming a relatively smooth appearance. In this whole process, fiber diameters have little change, as shown in Figure S5. The corresponding schematic diagram about this fine organization was shown in Figure S6. The removal of pectin and other amorphous constituents effect the rearrangement of the cellulose molecules, leading to better packing of cellulose chains and an increase in crystallinity (Figure S7), therefore improving the fiber strength. Interfacial friction formed between PVA and coir fiber increases with the increased surface roughness caused by NaOH treatment. In the process of tension, the axial tension and the interfacial friction force are a pair of interacting forces. Thus, with NaOH treatment, the strength was improved. This mechanism we put forward and demonstrated provides new ideas and references for the explanation of related problems in the future.

Figure 5 shows SEM images of typical structure in fiber before and after PVA infusion. Figure 5a is a ribbon helix. Due to being in place far from the center opening of fiber and having a quite wide and smooth surface, there is no obvious change in the ribbon helix morphology. Figure 5b,c shows cross

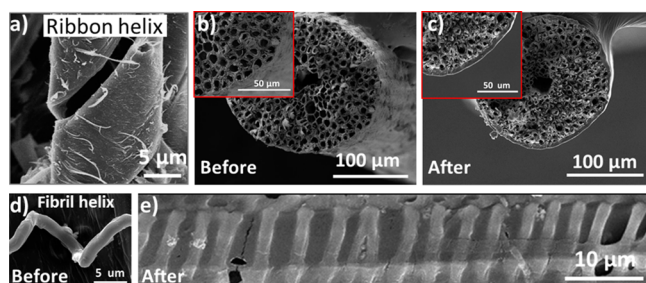


Figure 5. SEM images of typical structures of coir fiber before and after PVA infusion. (a) Ribbon helix showing no obvious change. (b and c) Cross sections of coir fiber revealing obvious PVA coating layer. Close views were shown in the insets of parts b and c. (d and e) Fibril helix showing long and continuous PVA coating. The coating of PVA plays a significant role in increasing the material strength and toughness.

sections of coir fiber before and after PVA immersion revealing an obvious PVA coating layer due to hydrophilicity and direct chemical adhesion. Close views were shown in the inset of Figure 5b,c. Figure 5d,e shows the fibril helix. The gap between each loop along with the parallel and aligned fibril skeleton renders a higher roughness to the integrated fibril helix compared with the ribbon helix. Thus, the fibril helix, with a higher roughness and existing near the center, was easily coated by PVA solution forming a long and continuous PVA coating layer (Figure 5e). Except for acting in the role of chemical interaction in the interface to improve the strength, the coating of PVA also plays a significant role in increasing the material toughness as a soft segment in large deformations.²³

Figure 6 shows the tensile fracture morphology exploring the mechanism about mechanical improvement. Figure 6a is an

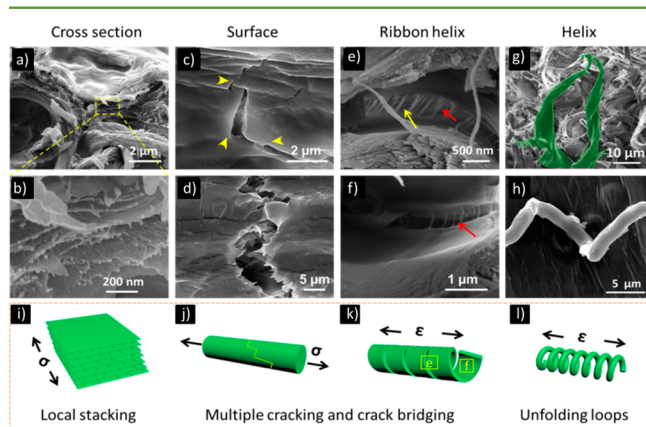


Figure 6. Fracture morphology of the coir fiber after alkali and PVA treatment. (a) Cross section of fiber tensile fracture edge. (b) Magnification of the dashed box in part a, forming a stacking and pulling out structure layer by layer between PVA, cellulose nanofibrils, and substrate. (c, d) Surface fracture morphology after tension. (c) Microcrack divergence. (d) Fibril pulling out, with polymer extension and fracture at the tip of a microcrack. (e, f) Crack bridging. (g, h) Unfolded morphology of two typical helices. (i–l) Corresponding schematic diagram.

SEM image of breaking at the elliptical pit after NaOH and PVA treatment, and a close view is shown in Figure 6b. A typical stacking structure layer by layer along the tensile direction was formed through PVA and cellulose nanofibrils at the nanometer scale. It is the perfect structure and chemically

sophisticated interaction that renders the fiber a large enhancement in strength. Figure 6c,d reveals fiber surface morphology after tension. The apparent characteristic is the microcrack divergence and crack extension (Figure 6c denoted as yellow) formed with large tensile strain. Also, with strain increasing, the cellulose fibrils were pulled out, and the fracture mode was formed (Figure 6d). Figure 6e,f shows fracture morphology outside and inside the surface of the helical ribbon, respectively. There are some bridging cracks obviously formed through cellulose nanofibrils, which is an important factor for toughness. By this means, energy dissipation pervades through a larger volume, rather than only at the fracture surface, resulting in integrated strength and toughness. Displayed in Figure 6g,h are helix structures after a break. The total absorbed energy consists of two parts: the unfolding of loops and the breakage of the unfolded backbone. In detail, in the process of tension, the loops (hidden length in helix) are stretched and unfolded, and carry the load gradually, thereby improving the toughness of fiber in comparison to the benchmark straight counterpart due to the energy necessary to straighten the helix. The bottom (Figure 6i–l) shows a corresponding typical fracture mechanism. This confluence of multiscale hierarchical microstructures is beneficial to improve both the strength and toughness.²⁴

Our strategy for fabricating a strong coir fiber composite of integrated strength and toughness compared with other engineering and natural fibers shows great advantages as shown in Figure 7. The density of the coir fiber is 1.15 g/cm³;

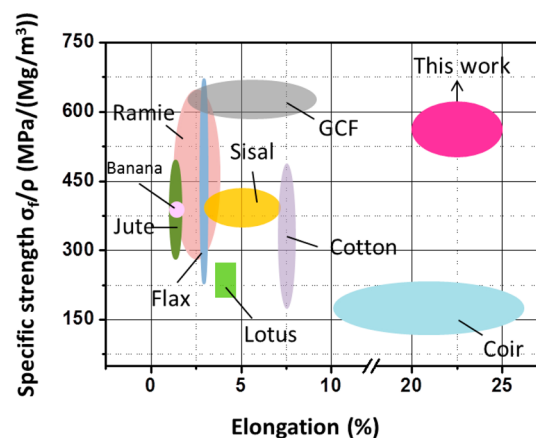


Figure 7. Diagram of specific strength versus elongation for comparing a range of engineering and natural fibers, such as ramie, GCF, sisal, flax, cotton, jute, hemp, lotus, and coir fibers.^{2,5}

the specific strength up to 610.40 MPa/(Mg/m³) [552.49 ± 57.91 MPa/(Mg/m³)] of our coir composite fiber is superior than that of other representative reported natural composite fibers.^{2,5} More importantly, the elongations of those fibers are in the range 1.16–8.50%,^{2,5} which are far lower than that of our single green composite fiber (22.51% in average), indicating better usability of our strong composite fiber.

CONCLUSIONS

In conclusion, allowing for the global environmental problems and inspired by the relationship of biology multiscale hierarchical structure and superior performance, we proposed a simple, low-cost alkali treatment and PVA injection approach that could fabricate coir/PVA composite fibers. The obtained

composite fiber shows strong integrated strength and toughness up to 635.36 ± 66.60 MPa and 83.14 ± 10.02 MJ m⁻³, which was superior to other natural fiber/polymer composites. Further, the mechanism for integrated strength and toughness was also demonstrated here. Because the compositions of most plant materials are basically the same, the proposed method for mechanical enhancement provides a versatile strategy for designing and developing new green materials with excellent strength and toughness.

■ ASSOCIATED CONTENT

Supporting Information

The Supporting Information is available free of charge on the ACS Publications website at DOI: 10.1021/acssuschemeng.6b00830.

SEM images, IR spectra, strength with NaOH concentration, fiber diameter changes, removing process, and XRD for mechanical enhancement mechanism (PDF)

■ AUTHOR INFORMATION

Corresponding Authors

*E-mail: wangn@buaa.edu.cn.

*E-mail: zhaoyong@buaa.edu.cn.

Notes

The authors declare no competing financial interest.

■ ACKNOWLEDGMENTS

The authors acknowledge the NSFC (21433012, 21374001, 21134003, and 21222309), 863 Program (2013AA032203), 973 Program (2012CB933200), the Program for New Century Excellent Talents in University of China, the Fundamental Research Funds for the Central Universities, and the China Scholarship Council (201406025059, 201506025110).

■ REFERENCES

- (1) Mohanty, A. K.; Misra, M.; Drzal, L. T. Sustainable biocomposites from renewable resources: opportunities and challenges in the green materials world. *J. Polym. Environ.* **2002**, *10*, 19–26.
- (2) (a) Zini, E.; Scandola, M. Green composites: An overview. *Polym. Compos.* **2011**, *32*, 1905–1915. (b) Cheung, H.; Ho, M.; Lau, K.; Cardona, F.; Hui, D. Natural fibre-reinforced composites for bioengineering and environmental engineering applications. *Composites, Part B* **2009**, *40*, 655–663.
- (3) (a) Mohammadinejad, R.; Karimi, S.; Iravani, S.; Varma, R. S. Plant-derived nanostructures: types and applications. *Green Chem.* **2016**, *18*, 20–52. (b) Anastas, P. T.; Lankey, R. L. Sustainability through Green Chemistry and Engineering. *ACS Symp. Ser.* **2002**, *823*, 1–11.
- (4) Gerbode, S. J. How the Cucumber Tendril Coils and Overwinds. *Science* **2012**, *337*, 1087–1091.
- (5) Wu, M.; Shuai, H.; Cheng, Q.; Jiang, L. Bioinspired green composite lotus fibers. *Angew. Chem., Int. Ed.* **2014**, *53*, 3358–61.
- (6) Meyers, M. A.; McKittrick, J.; Chen, P. Structural Biological Materials: Critical Mechanics Materials Connections. *Science* **2013**, *339*, 773–779.
- (7) Hu, L.; Pasta, M.; Mantia, F. L.; Cui, L.; Jeong, S.; Deshazer, H. D.; Choi, J. W.; Han, S. M.; Cui, Y. Stretchable, porous, and conductive energy textiles. *Nano Lett.* **2010**, *10*, 708–714.
- (8) (a) Wang, J. S.; Wang, G.; Feng, X. Q.; Kitamura, T.; Kang, Y. L.; Yu, S. W.; Qin, Q. H. Hierarchical chirality transfer in the growth of Towel Gourd tendrils. *Sci. Rep.* **2013**, *3*, 3102. (b) Chen, P.; Xu, Y.; He, S.; Sun, X.; Pan, S.; Deng, J.; Chen, D.; Peng, H. Hierarchically arranged helical fibre actuators driven by solvents and vapours. *Nat. Nanotechnol.* **2015**, *10*, 1077–83.
- (9) Mohanty, A. K.; Misra, M.; Drzal, L. T. Surface modifications of natural fibers and performance of the resulting biocomposites: An overview. *Compos. Interfaces* **2001**, *8*, 313–343.
- (10) Li, Y. Q.; Samad, Y. A.; Polychronopoulou, K.; Alhassan, S. M.; Liao, K. Carbon Aerogel from Winter Melon for Highly Efficient and Recyclable Oils and Organic Solvents Absorption. *ACS Sustainable Chem. Eng.* **2014**, *2*, 1492–1497.
- (11) Wegst, U. G.; Bai, H.; Saiz, E.; Tomsia, A. P.; Ritchie, R. O. Bioinspired structural materials. *Nat. Mater.* **2015**, *14*, 23–36.
- (12) (a) Zheng, Y.; Bai, H.; Huang, Z.; Tian, X.; Nie, F. Q.; Zhao, Y.; Zhai, J.; Jiang, L. Directional water collection on wetted spider silk. *Nature* **2010**, *463*, 640–3. (b) Lazaris, A.; Arcidiacono, S.; Huang, Y.; Zhou, J. F.; Duguay, F.; Chretien, N.; Welsh, E. A.; Soares, J. W.; Karatzas, C. N. Spider silk fibers spun from soluble recombinant silk produced in mammalian cells. *Science* **2002**, *295*, 472–476. (c) Partlow, B. P.; Hanna, C. W.; Rnjak-Kovacina, J.; Moreau, J. E.; Applegate, M. B.; Burke, K. A.; Kaplan, D. L.; et al. Highly tunable elastomeric silk biomaterials. *Adv. Funct. Mater.* **2014**, *24*, 4615–4624.
- (13) (a) Brown, C. P.; Harnagea, C.; Gill, H. S.; Price, A. J.; Traversa, E.; Licoccia, S.; Rosei, F. Rough fibrils provide a toughening mechanism in biological fibers. *ACS Nano* **2012**, *6*, 1961–1969. (b) Studart, A. R. Biological and bioinspired composites with spatially tunable heterogeneous architectures. *Adv. Funct. Mater.* **2013**, *23*, 4423–4436.
- (14) John, M.; Thomas, S. Biofibres and biocomposites. *Carbohydr. Polym.* **2008**, *71*, 343–364.
- (15) (a) Ritchie, R. O. The conflicts between strength and toughness. *Nat. Mater.* **2011**, *10*, 817–22. (b) Bouville, F.; Maire, E.; Meille, S.; Van de Moortele, B.; Stevenson, A. J.; Deville, S. Strong, tough and stiff bioinspired ceramics from brittle constituents. *Nat. Mater.* **2014**, *13*, 508–14.
- (16) Nagarajan, V.; Mohanty, A. K.; Misra, M. Sustainable Green Composites: Value Addition to Agricultural Residues and Perennial Grasses. *ACS Sustainable Chem. Eng.* **2013**, *1*, 325–333.
- (17) Bismarck, A.; Aranberri-Askargorta, I.; Springer, J.; Mohanty, A. K.; Misra, M.; Hinrichsen, G.; Czaplá, S. Surface characterization of natural fibers; surface properties and the water up-take behavior of modified sisal and coir fibers. *Green Chem.* **2001**, *3*, 100–107.
- (18) Haque, M. M.; Hasan, M.; Islam, M. S.; Ali, M. E. Physico-mechanical properties of chemically treated palm and coir fiber reinforced polypropylene composites. *Bioresour. Technol.* **2009**, *100*, 4903–6.
- (19) Nam, T. H.; Ogihara, S.; Tung, N. H.; Kobayashi, S. Effect of alkali treatment on interfacial and mechanical properties of coir fiber reinforced poly(butylene succinate) biodegradable composites. *Composites, Part B* **2011**, *42*, 1648–1656.
- (20) Mohanty, A. K.; Rout, J.; Tripathy, S. S.; Misra, M.; Nayak, S. K. The influence of fibre treatment on the performance of coir-polyester composites. *Compos. Sci. Technol.* **2001**, *61*, 1303–1310.
- (21) Rosa, M. F.; Chiou, B. S.; Medeiros, E. S.; Wood, D. F.; Williams, T. G.; Mattoso, L. H.; Orts, W. J.; Imam, S. H. Effect of fiber treatments on tensile and thermal properties of starch/ethylene vinyl alcohol copolymers/coir biocomposites. *Bioresour. Technol.* **2009**, *100*, 5196–202.
- (22) Cai, M.; Takagi, H.; Nakagaito, A. N.; Katoh, M.; Ueki, T.; Waterhouse, G. I. N.; Li, Y. Influence of alkali treatment on internal microstructure and tensile properties of abaca fibers. *Ind. Crops Prod.* **2015**, *65*, 27–35.
- (23) Naraghi, M.; Filleter, T.; Moravsky, A.; Locascio, M.; Loutfy, R. O.; Espinosa, H. D. A multiscale study of high performance double-walled nanotube polymer fibers. *ACS Nano* **2010**, *4*, 6463–6476.
- (24) (a) Usov, I.; Mezzenga, R. Correlation between nanomechanics and polymorphic conformations in amyloid fibrils. *ACS Nano* **2014**, *8*, 11035–11041. (b) Shang, Y.; Li, Y.; He, X.; Du, S.; Zhang, L.; Shi, E.; Wu, S.; Li, Z.; Li, P.; Wei, J.; Wang, K.; Zhu, H.; Wu, D.; Cao, A. Highly twisted double-helix carbon nanotube yarns. *ACS Nano* **2013**, *7*, 1446–1453.